NASA TM X-73554

NASA TECHNICAL MEMORANDUM

NASA TM X-73554

ELECTRON BOMBARDMENT PROPULSION SYSTEM CHARACTERISTICS FOR LARGE SPACE SYSTEMS

by D. C. Byers and V. K. Rawlin
Lewis Research Center
Cleveland, Ohio 44135

TECHNICAL PAPER to be presented at the
Twelfth International Electric Propulsion Conference sponsored by the
American Institute of Aeronautics and Astronautics
Key Biscayne, Florida, November 15-17, 1976

Presented are the results of an analysis of electron bombardment ion propulsion systems for use in the transportation and on-orbit operations of large space systems. Using baseline technology from the ongoing primary propulsion program and other sources, preliminary estimates of the expected characteristics of key system elements such as thrusters and propellant storage systems have been performed. Projections of expected thruster performance on argon are presented based on identified constraints which limit the achievable thrust and/or power density of bombardment thrusters. System characteristics are then evaluated as a function of thruster diameter and specific impulse.

E-8992

ELECTRON BOMBARDMENT PROPULSION SYSTEM CHARACTERISTICS FOR LARGE SPACE SYSTEMS

by D. C. Byers and V. K. Rawlin

Lewis Research Center

INTRODUCTION

The application of electron-bombardment ion thruster subsystems has been analyzed in detail for a broad set of planetary[1-4] and near earth[5, 6] missions. The thrust subsystems assumed for contemporary studies employed the 30-cm diameter mercury bombardment ion thruster[7] presently under development by the National Aeronautics and Space Administration. In general, these studies assumed shuttle sized (or smaller) payloads.

Recently, studies have been performed on the characteristics and potentials of Large Space Systems (LSS) which are significantly larger in final configuration than shuttle size payloads.[8, 9, 10] Examples of such systems are satellite power stations [8, 9] space manufacturing facilities, [10] and very large communication systems. Propulsion requirements for these systems have been analyzed in some detail.[11, 12] These studies have indicated that the propulsion system characteristics can very strongly impact the performance and cost of LSS. In particular, significant benefits are obtained by the use of high (>1500 seconds) specific impulse propulsion for the orbit-to-orbit transportation function. For example, large cost savings accrue[11] from the use of high specific impulse propulsion because of the reduction in orbit transfer propellant that is required to be raised from earth to low earth orbit (LEO). The on-orbit propulsion requirements have also been analyzed[13] and the potential benefits of high specific impulse propulsion for on-orbit propulsion are analogous to those identified for the orbit transfer transportation function.

Several candidate propulsion concepts have been proposed for use with

E-8992

STAR category 16
NASA TM X-73554
AIAA 76-1039

LSS. These include electron-bombardment thrusters[7]; magneto-plasmadynamic thrusters[14]; high specific impulse resisto jets; and thermal rockets where the on board propellant is heated by remotely based lasers.[15] Of these propulsion concepts, the electron-bombardment thruster is in the most advanced state of development and is capable of operation at the highest values of specific impulse.

The strong dependence of overall LSS performance and cost as a result of the propulsion subsystem characteristics was previously noted. Accurate projection of system benefits are difficult to assess unless the thrust subsystem characteristics are established.

This paper will discuss and evaluate some of the critical performance characteristics of electron-bombardment subsystems that are pertinent to the design of LSS. A brief review of LSS propulsion requirements will be presented to aid the selection of key concept options. A discussion follows on the selection and storage requirements of thruster propellant. Analysis of the expected performance and characteristics of bombardment thrusters is then presented followed by a brief discussion of power processing requirements for the proposed thrust subsystem approaches.

LSS PROPULSION REQUIREMENTS

The selection of thrust subsystem design and operating characteristics will ultimately depend, of course, on the ability of a particular propulsion subsystem to satisfy the overall system requirements. These requirements will include the usual propulsion performance parameters such as specific impulse, thrust, lifetime, and system dry mass and volume. In addition, many other characteristics such as potential ecological impact, availability of materials, refurbishment capability, and propulsion system cost will likely be of extreme concern for the scale of propulsion subsystems required for LSS.

The propulsion subsystem requirements will be sensitive to system approach options.[11, 12] These options include the degree of LEO assembly assumed, constraints on transportation trip time, launch and orbit transfer

strategy, orbit transfer and on-orbit payload design, power source assumptions, and on-orbit design lifetime. Detailed consideration of such options is beyond the scope of this paper. However, for completeness and to direct the selection of critical design options for proposed electron-bombardment thruster subsystems a brief review of the propulsion requirements of LSS is presented.

Orbit transfer requirements may be estimated by use of the rocket equation:

$$M_P = M_F\left(e^{\Delta V/I_{sp}g} - 1\right) \tag{1}$$

where

M_P is propellant mass, kg

M_F is payload mass, kg

ΔV is the mission velocity increment, m/sec

I_{sp} is the specific impulse, sec.

g, is the acceleration due to gravity, 9.8 m/sec^2

This equation ignores many factors such as occultation, attitude control requirements during transfer, and penalties associated with low versus high thrust. For the purposes of this paper, however, use of this equation is felt adequate. Figure 1 shows the required propellant for orbit transfer as a function of payload mass with specific impulse as a parameter.

The standard thrust and power equations were used with equation 1 to give the following equations.

$$T = \frac{M_F}{\Delta t}\, e^{\Delta V/I_{sp}g} - 1 \quad 1.1574\times10^{-5}\, I_{sp}g \tag{2}$$

and

$$\eta_T P = \frac{M_F}{\Delta t}\left(e^{\Delta V/I_{sp}g} - 1\right)(1.1574\times10^{-5})\,\frac{(I_{sp}g)^2}{2} \qquad (3)$$

where

T is the thrust, N

Δt is the thrusting time, days

η_T is the thrust subsystem efficiency

P is the thrust subsystem power, W

Figures 2 and 3 show the required total thrust and the product of the thrust subsystem efficiency and the required total power as functions of the ratio of payload mass to trip time. For figures 1, 2, and 3 a ΔV of 5770 meters per second was assumed, which corresponds to the total impulse requirement for orbit transfer from 352 kilometers to geosynchronous altitude with a 28.5 degree plane change, to account for the Shuttle orbit plane inclination.

Figure 1 shows the strong dependence of propellant mass on specific impulse. As seen on figure 2, the thrust is most sensitive to the ratio of payload mass to trip time and above about 2000 seconds the thrust is quite insensitive to specific impulse. Figure 3 shows the approximately linear increase in required power with specific impulse.

The requirements shown on figures 1, 2, and 3 differ primarily in scale from those for missions for which the 30-cm mercury bombardment thruster has been developed. As an example, one of the more energetic proposed planetary missions is the mercury orbiter which requires about 1330 kg[1] of mercury propellant and a 25 kW solar cell power source. If proposed concepts such as the raising of significant portions of an assembled space power satellite were carried out, the propellant, thrust, and power requirements are simply larger in magnitude than for the mercury orbiter mission. To a further highlight this comparison, figure 4 shows the number of baseline design 30-cm mercury thrusters required for the selected transfer mission as a function of the ratio of payload mass to trip time.

On-orbit propulsion requirements for a 11.4 kg satellite were analyzed

in reference 13. Table I shows the on-orbit propellant requirements derived by this study along with the approximate number of standard 30-cm mercury thrusters (138.3 kg/yr propellant flow rate at a specific impulse of 2840 sec) required to satisfy each on-orbit propellant requirement. Additional thrusters or reconfiguration of thrusters may be necessary to perform certain control functions such as longitudinal stationkeeping or that due to microwave pressure. For a satellite with a 30 year lifetime the number of 15,000 hour lifetime thrusters required would increase by a factor of 18.

It is of interest to compare the on-orbit and orbit raising propulsion requirements. This was done by using the on-orbit propellant requirements of reference 13, without the propellant requirements to counteract the output microwave power or correct for orbit eccentricity drift due to solar pressure. The orbit transfer propellant requirements of that satellite were calculated for a variety of transfer times. Figure 5 shows the ratio of the required propellant flowrates for on-orbit and orbit transfer propulsion as a function of orbit transfer time. Figure 6 shows the ratio of total impulses for on-orbit and orbit transfer as a function of on-orbit lifetime. For reasons discussed later, the specific impulse was selected to be 13,000 seconds; however, the comparisons shown on figures 5 and 6 are not very sensitive to specific impulse variations in this range (fig. 2).

Figure 5 shows that, for a given LSS, the on-orbit propellant flow rates (and thrusts) are much smaller than for the orbit transfer phase. However, figure 6 shows that for LSS lifetimes of interest[11] (about 30 years) the on-orbit total impulse is nearly equal to the total impulse required for orbit transfer. Exact comparisons of the types shown on figures 5 and 6 will depend, of course, on the specific system and selected propulsion strategy. Optimal selection of the propulsion subsystem must, however, consider both the orbit transfer and on-orbit propulsion phases.

PROPELLANT SELECTION AND STORAGE

Propellant Selection

Bombardment thrusters have been operated successfully over a wide

range of conditions with a large variety of propellants.[16] Elemental propellants ranging in mass from hydrogen to mercury have been tested along with some heavy molecules. Thruster performance as a function of propellant has been discussed and theoretical considerations presented by many authors[17, 18] with a review by Kaufman[17] being one of the most general and recent.

Based on the magntitude of requirements shown in figure 1, it is the opinion of the authors that propellant selection will be driven by the constraints of propellant availability, ecological impact, and cost. For this reason it was decided to first select a propellant appropriate for use with LSS. Subsequently, storage penalties and thruster performance with the selected propellant will be discussed.

From the standpoint of availability, no clear choice of propellant was vident as many candidates are available from terrestial or atmospheric sources.

The impact of environmental considerations is less straightforward. The velocity of any propellant ion emerging from a bombardment thruster operated in ranges of interest would be well above earth escape velocity. The disposition of the accelerated ions is, however, uncertain due to such effects as the earths magnetic field, collisions, and collective charge phenomena in the atmosphere. In addition, about ten percent of the total propellant will escape the thrust subsystem as slow neutrals with velocities well below earth escape velocity. The impact, if any of released propellant has not been defined.

The authors elected to consider only propellants available from the earths atmosphere in order to minimize potential ecological impact. Table II shows the constituency of the atmosphere.[19] If the further constraints of no known toxicity in element or combined form along with low reactivity with atmospheric constituents are adopted, a natural choice of one of the inert gases shown on Table II follows.

Bombardment thrusters have been extensively operated[16] on argon, krypton, and xenon. All are acceptable from the standpoint of compatibility with known thruster design concepts. To select a propellant, the cost of the three gases was reviewed and is shown on Table III with the cost of argon

normalized to unity. Studies such as reference 11 indicate that the cost of argon propellant is a small (less than one percent) fraction of overall transportation system cost. Use of higher cost propellants such as krypton or xenon would, however, significantly impact overall system economics.

From the above, argon was selected as the baseline propellant for use with LSS bombardment thruster subsystems. It should be stressed that if either krypton or xenon costs were reduced to that of argon, strong consideration should be given to their use. The efficiency of thruster operation with either propellant would be improved over that with argon. In addition, the thrust to power ratio and specific impulse would vary nearly directly and inversely, respectively, as the square root of the ratio of the propellant mass to the mass of argon.

Propellant Storage

To fully describe the impact of selection of a particular propellant it is necessary to evaluate the storage penalties associated with that propellant. A brief review of pertinent data was made with the object of providing a rough estimate of storage requirements with argon propellant.

Propellant storage has been the subject of intense development for many years.[20] Concepts for storage of liquid hydrogen and liquid oxygen have been systemmatically studied and developed for chemical rocket systems. The thermodynamic vent/screen baffle cryogenic storage system (hereinafter called TCSS) is one such concept.[21] Figure 7 shows some details of a TCSS and operation is described in detail in reference 21. This concept includes a vacuum jacket, and outflow of propellant is used for cooling purposes.

A preliminary analysis was performed to estimate the tankage mass with argon propellant.[22] A tank capable of holding 20,000 kg of liquid argon at 1.4×10^5 N/m^2 (20 psia) was assumed and a mass breakdown is given in Table IV. A steady argon output flow of 5×10^{-5} kg/sec for the purpose of cooling was assumed and was found adequate to balance all expected thermal

inputs to the propellant tank. The required propellant flow rate for cooling purposes will vary with tank size. The very large ratio of propellant mass to required coolant rate of propellant (about 0.4×10^9 seconds for the design point) indicates that the TCSS concept could be used with negligible propellant loss without the requirement of active cooling systems.

Figure 8 shows the tankage mass fraction obtained by extrapolation of the single point design of reference 22. This extrapolation was made by assuming that the ratio of the masses of propellant to tankage scaled directly as the diameter of the tank. As seen in figure 8 tankage mass fractions less than 3.7 percent can be obtained for propellant loads greater than 20,000 kg.

THRUSTER PERFORMANCE AND CHARACTERISTICS

General Description

The 30-cm diameter engineering model thruster (EMT) has been developed for use with mercury propellant. Detailed descriptions of the design and operation of this thruster have been given elsewhere[17, 18] and the following discussion will be directed at describing the expected characteristics of argon bombardment thrusters.

The critical features of the thruster are inlet propellant electrical isolation and flow regulation systems; a cathode which emits electrons to bombard and ionize the neutral propellant; a discharge chamber with a shaped magnetic field where the propellant is ionized; an ion acceleration system consisting of two grids; a neutralizer, which emits an electron current equal to the ion beam current to maintain ion beam neutrality; and a shield surrounding the thruster to prevent electrical interactions with the local plasma.

The performance of several different size bombardment thrusters operated with argon has been reported in references 16, 23, 25, and 25. In general, operation of the thruster with argon was similar to that with mercury. The discharge chamber losses, expressed as energy per beam ion (ϵ_I), were similar for both propellants, but the propellant utilization efficiency (η_u), was

always lower with argon. When investigated, the ion extraction capability of the grid system varied inversely with the mass of the ion used, as expected.

Performance and Limitations

Many features of the thruster, such as the structure, insulators and cabling are passive and would not impact the performance of a thruster operated on argon. Those features which would be expected to contrain thruster performance or require modifications for operation with argon will be discussed below.

Ion Accelerator System

The accelerator system consists of two grids with many circular holes. The upstream grid (screen) is charged positively to provide the approximate net ion accelerating voltage while the downstream grid (accelerator) is charged negatively to prevent the neutralizing electrons from entering the discharge chamber. The sum of the absolute values of the screen and accelerator voltages is called the total accelerating voltage.

The accelerator system imposes a basic limitation on the power and thrust densities that may be obtained with a bombardment thruster. This limit arises from the fact that for any accelerator system configuration and grid spacing there exists a maximum ion current (or current density) which may be extracted as a function of the voltage applied between the two grids. This is often referred to as the "perveance limit." The maximum ion current increases strongly with increasing applied voltage, decreasing grid spacing and nearly directly with the screen grid open area. Recently, Sovey[25] has experimentally determined a relationship which predicts the maximum ion current density (for Argon, Xenon and Mercury) for grid systems which are near the minimum spacing expected to be attainable for large dished grid systems. Assuming operation at a maximum ratio of net-to-total ion accelerating voltage of 0.9 and a screen grid open area fraction of 0.7, Sovey's relationship for argon propellant may be expressed as:

$$\frac{J_B}{d^2} = 0.63 \cdot 10^{-9} V_N^{2.25} \qquad (4)$$

where

J_B is the beam current, A

d is the thruster diameter, cm

V_N is the net accelerating voltage, V

In equation 4, it is seen that the beam current density rises very strongly with increasing net accelerating voltage. Earlier discussions stressed the desire to operate at high values of specific impulse (I_{sp}) which is proportional to the square root of V_N. But V_N cannot be increased without limit because there is, for any given grid spacing, a maximum total accelerating voltage which may be applied to the grids without continuous high voltage breakdowns. While the maximum allowable V_N increases as the grid spacing is increased, the beam current density of equation 4 decreases because it is inversely proportional to approximately the square of the grid spacing. In addition, the maximum field strength decreases, as the grid spacing is increased, at a rate such that maximum value of beam current density occurs at the minimum possible grid spacing. For the near-minimum spacing of 0.6 mm, the value used for equation 4, the maximum value of V_N was assumed to be 5000 v which corresponds to an I_{sp} of about 13,000 seconds at a propellant utilization efficiency (η_u) of 0.82.

Discharge Power

The major power loss of the thruster occurs in the discharge chamber where a large fraction of the discharge power is lost by radiation to and particle collisions with the discharge chamber walls. Heating of passive thruster components, cathodes and grids excluded, can limit thruster operation only if component temperatures reach the limits of structural or chemical integrity. It has been shown by Sovey[25] that cathodes can be designed

to operate at temperatures commensurate with long lifetimes at elevated emission current levels required by thrusters operated at high beam currents. In addition, when necessary, multiple cathodes may be used for larger thrusters.

The only active component expected to limit thruster performance as a result of elevated discharge power levels is the ion acceleration system. Tests of mercury bombardment thrusters with diameters up to 150 cm[26] have been conducted in which the ion acceleration grid temperatures and discharge powers used were noted. Analysis of these data show that the measured average temperature of the grid set was nearly equal to the average temperature obtained when it was assumed that one-fourth of the total discharge power was absorbed by the grids which in turn radiated heat with an emissivity of 0.4. Applying these assumptions to an argon bombardment thruster operating with an ϵ_I of 200 leads to the following expression for the maximum beam current density:

$$\frac{J_B}{d^2} = 2.507\times10^{-14}(\overline{T})^4 \qquad (5)$$

where $\overline{T}$ is the maximum allowable average temperature, assumed for the grid set, in ^{o}K. Thus, for a selected average grid temperature, the beam current density limit is constant. At the beam current density determined by equation 4 for a V_N of 5000 volts, the maximum allowable $\overline{T}$ would be 1513^{o} K. Because the grids are made of molybdenum, there does not appear to be a materials problem even at these elevated temperatures. Reference values of creep[27, 28] indicate negligible dimensional changes even at temperatures of 1900^{o} K over several hundred thousands of hours.

Dished grids were designed to move in a predetermined axial direction when they were subjected to changes in temperature. Use of the equations presented in reference 29 indicate that the reductions in grid-to-grid spacings resulting from hotter grid temperatures can easily be eliminated by increasing the dish depth during fabrication. In addition, there are no requirements for radiators to cool the thruster components. Although there are no known problems at these elevated temperatures, operation at discharge power levels which would lead to grid temperatures of 1500^{o} K remains to be demonstrated. Therefore, for this study, the maximum allowable $\overline{T}$ was arbi-

trarily chosen to be 913° K (700° C), less than a factor of two greater than the temperatures of the present EMT.

Thruster Performance

Figure 9 shows how the ratio of specific impulse to propellant utilization efficiency (I_{sp}/η_u) varies with V_N for argon propellant. Figure 10 shows the three ion accelerating system operating limitations for a grid spacing of 0.6 mm. The "perveance" limit (eq. 4) determines the minimum value of V_N required to obtain a given beam current density. At a value of V_N of 2274 volts, or I_{sp}/η_u of about 11,000 seconds, the maximum average grid temperature limit of 700° C limits the ratio of beam current to square of thruster diameter to 0.0225 amp/cm^2. The maximum field strength limit specifies practical maximum values of V_N of 5000 volts or I_{sp}/η_u of near 16,000 sec. This maximum in specific impulse is a result of the assumption of close spaced ion accelerator grids. This assumption was adopted because the maximum thrust density (and hence, the minimum number of thrusters for a particular thrust level) is achieved with closed spaced accelerator grids. Specific impulses in excess of 16,000 seconds can be obtained with thrusters which use large spaced grids and values up to 25,000 seconds have been demonstrated with mercury propellant[30] (equivalent to about 55,000 seconds with argon). Use of large spaced grids does, however, strongly limit the thrust density and for that reason was not considered herein.

Using the beam current density limitations of figure 10, the thrust and power density limitations were calculated and are shown in figures 11 and 12, respectively, as functions of the ratio of specific impulse to propellant utilization efficiency. For values of I_{sp}/η_u less than 11,000 sec, both parameters decrease rapidly as the I_{sp}/η_u is decreased. As the value of I_{sp}/η_u is increased from 11,000 sec to 16,000 sec, the thrust and power densities continue to increase but at a slower rate.

As the power to the thruster increases the discharge and fixed power losses become nearly negligible when compared to the beam power so that

the total thruster efficiency approaches the propellant utilization efficiency. This is shown in figure 13 where the total efficiency is plotted as a function of specific impulse. The thruster performance presented in this section has not been corrected for expected thrust losses such as beam divergence and multiply-charged ions. It is expected that those correct ions would result in decreases in thruster efficiency between about 5 to 10 percent.

Thruster Scaling

Bombardment thrusters with diameters of 2.5, 5, 8, 10, 15, 20, 30, 50 and 150 cm have been tested at Lewis Research Center. Whenever the size of the thruster was varied, the performance obtained at that particular time was nearly as expected based on developed scaling laws. The improvements in thruster performance, which have occurred over the years, have been successfully applied to thrusters of different size than those for which the improvement first occurred.

Performance

Most bombardment thrusters are cylindrical in shape and therefore their volume may be defined by a length and a diameter. In addition, Kaufman[17] has noted that optimized thruster length changes little as the diameter is varied. Thus, to scale the operating or performance parameters of various size thrusters only the diameter need be varied.

Presently, 8[31] and 30[7] cm diameter thrusters are at an advanced stage of development. Since this represents nearly a four-to-one increase in thruster diameter with less than a 50 percent increase in thruster length, it is expected that the thruster diameter may be increased to 100 cm with minor performance variations. The major modifications would be expected to occur with cathodes and ion extraction systems. Thrusters larger than 50 cm diameter would probably use multiple cathodes for improved lifetime, reliability, and performance. The use of dished grids to maintain a close spacing over a

30 cm diameter has proven to be quite successful. Presently, there does not appear to be any technological reasons to prohibit the fabrication of dished grids with diameters up to 100 centimeters in diameter (although materials such as molybdenum do not presently appear to be available in such sizes).

Figures 14 and 15 show the expected maximum thrust and power per thruster as a function of thruster diameter. Also, figure 16 shows the number of various size thrusters required to perform orbit transfer functions as a function of the ratio of payload mass to trip time. The number of 100 cm argon thrusters required for a particular mission is about 1130 times less than the required number of 30 cm mercury thrusters (fig. 4). The on-orbit propellant requirements for the satellite studied in reference 13 using a propulsion subsystem with an I_{sp} of 13,000 sec would be only 62 percent of those given in Table I.

MASS

The mass per thruster as a function of thruster diameter was estimated by applying the following assumptions. For large space systems, the use of a shuttle launch vehicle and new packaging techniques were assumed which permitted substantial reductions in the masses of structural components. Mass reductions were also assumed when the massive high voltage propellant isolators required with mercury propellant were redesigned for use with argon. With the use of these assumptions the mass of a 30 cm diameter thruster was reduced from 8.2 kg (mercury EMT) to about 3.8 kg. The thruster components were then separated into four groups with masses which were either fixed, varied with thruster diameter or the square of diameter; or varied in discrete increments as the thruster size increased, such as multiple cathodes. The thruster diameter was then varied and component masses were computed to obtain figure 17 which gives the estimated thruster mass as a function of thruster diameter.

Power Conditioning

The thruster power conditioning requirements and characteristics are strongly influenced by the mission and the power source selected and will therefore be discussed only briefly. The input power to the thruster consists of three major elements: the beam (ion acceleration) power, the discharge (propellant ionization) power, and a small amount of additional (other) power used to control the thruster which experience has shown is relatively insensitive to thruster size. The relative magnitudes of these powers are shown on Table V for the baseline 30-cm engineering model thruster (EMT) with mercury propellant and also for a 60 cm argon thruster at two values of specific impulse. As shown in Table V, the beam power is the major power demand of a thruster with the discharge power next. The other, nearly fixed, losses represent a negligible fraction of the thruster power, especially at high specific impulse.

All thruster input power is conditioned with the baseline 30-cm EMT system.[32] The resultant power conditioning specific mass, including thermal control for the power conditioner, is about 13 mg/kW for each 3 kW thruster system. Some estimates have been presented in reference 33 of the characteristics of electric propulsion power conditioning to be expected in the future for large (up to 1000 kW) systems. Reference 33 indicated that reductions in specific mass ranging from about a factor of three to a factor of 10 might be expected in the time scale between the years 1985 and 2000.

Another approach has been demonstrated which could more drastically reduce the power conditioning requirements. For the approach, the ion beam power was obtained directly from a solar array on 8[34], 15[35] and 30[36] cm electron bombardment mercury thrusters. The discharge was also operated directly from an array for 15[35] and 30[36] cm thrusters. The operation of the beam and discharge from an array was accomplished in a straight-forward fashion in all cases and the characteristics of the solar array output (such as low-ripple and inherent current limited output) were well matched to the thruster requirements. When applied to a 60 cm argon thruster, direct operation from a solar array would require conditioning of only about 100 watts of power (Table V) thereby reducing the specific mass of the thrust subsystem.

CONCLUDING REMARKS

LSS propulsion requirements are far beyond those for which the present electron bombardment thruster systems are being developed. A review of those requirements indicated that a propellant other than mercury be selected. Argon was selected, based on availability, potential environmental impact, and present costs. Estimates of propellant storage requirements for argon were reviewed and found to be a small fraction of the propellant mass.

The performance characteristics of electron bombardment thrusters operated on argon were reviewed and limitations discussed. The maximum values of output thrust was found to be very sensitive to the specific impulse selected and limited by the perveance, temperature or breakdown characteristics of the ion accelerating system. Projection of the expected thruster performance and mass as a function of thruster diameter were presented. Finally, a brief review of present and potential advanced power conditioning was presented.

REFERENCES

1. Atkins, K. L., "Mission Applications of Electric Propulsion," AIAA Paper 74-1085, San Diego, Calif., 1974.

2. Duxbury, J. H. and Finke, R. C., "A Candidate Mission Using the Shuttle and Solar Electric Propulsion," AAS Paper 75-163, Denver, Colo., 1975.

3. Guttman, C. H., et al., "The Solar Electric Propulsion Stage Concept for High Energy Missions," AIAA Paper 72-465, Bethesda, M. D., 1972.

4. Sauer, C., "Trajectory Analysis and Performance for SEP Comet Encke Missions," AIAA Paper 73-1059, Lake Tahoe, Nev., 1973.

5. "Payload Utilization of SEPS," Boeing Aerospace Co. Rept. D-180-19783-1, July 1976.

6. "Concept Definition and Systems Analysis Study for a Solar Electric Propulsion Stage," Rockwell International Rept. SD74-SA-0176-1, Feb. 1975.

7. Schnelker, D. E. and Collett, C. R., "30-Cm Engineering Model Thruster Design and Qualification Tests," AIAA Paper 75-341, New Orleans, La., 1975.

8. Glaser, P. E., "Evolution of the Satellite Solar Power Station SSPS Concept," Journal of Spacecraft and Rockets, Vol. 13, 1976, pp. 573-576.

9. Grey, J., "The Outlook for Space Power," Astronautics & Aeronautics, Vol. 14, 1976, pp. 29-36.

10. O'Neill, G. K., "Engineering a Space Manufacturing Center," Astronautics & Aeronautics, Vol. 14, Oct. 1976, pp. 20-28.

11. "Initial Technical, Environmental, and Economic Evaluation of Space Solar Power Concepts," Vols. I and II, NASA Johnson Space Center Rept. JSC-11568, Aug. 1976.

12. Stearns, J. W., "Large-Payload Earth-Orbit Transportation with Electric Propulsion," Jet Propulsion Laboratory, Technical Memo 33-793, Sept. 1976.

13. Nathan, A., "Space-based Solar Power Conversion and Delivery Systems (Study)" Grumman Aerospace Corp. Rept. NSS-P-76-006, Oct. 1975.

14. Esker, D. W., Kroutil, J. C., and Checkley, R. J., "Radiation Cooled MPD Arc Thruster," McDonnell-Douglas Corp. Rept MDC-H296, July 1969; also NASA CR-72557.

15. Moeckel, W. E., "Optimum Exhaust Velocity for Laser-Driven Rockets," Journal of Spacecraft and Rockets, Vol. 12, 1975, pp. 700-701.

16. Byers, D. C. and Reader, P. D., "Operation of an Electron-Bombardment Ion Source Using Various Gases," NASA TN D-6620, 1971.

17. Kaufman, H. R., "Technology of Electron-Bombardment Ion Thrusters," in Advances in Electronics and Electron Physics, Vol. 36, Academic Press, Inc., New York, 1974, pp. 265-373.

18. Milder, N. L., "A Survey and Evaluation of Research on the Discharge Chamber Plasma of Kaufman Thrusters," Journal of Spacecraft and Rockets, Vol. 7, 1970, pp. 641-649.

19. Hodgman, C. D., ed., Handbook of Chemistry and Physics, 34th ed., Chemical Rubber Publ., Co., Cleveland, 1952.

20. Stark, J. A., et al., "Fluid Management Systems Technology Summaries," General Dynamics/Convair Rept. CASD-NAS-74-068, Dec. 1974; also NASA CR-134748.

21. Cady, E. C., "Design and Evaluation of Thermodynamic Vent/Screen Baffle Cryogenic Storage System for Space Shuttles, Space Tugs, and Spacelab," McDonnell Douglas Astronautics Co. Rept. MDC-G5979, June 1975; also NASA CR-134810.

22. Cady, E. C., McDonnell Douglas Astronautics Co. Huntington Beach, Calif.; Private Communication, 1975.

23. Reader, P. D., "The Operation of an Electric Bombardment Ion Source with Various Gases," in First International Conference on Electron and Ion Beam Science and Technology, R. Bakish, ed., Wiley, New York, 1965, pp. 925-935.

24. Schertler, R. J., "Preliminary Results of the Operation of a SERT II Thruster on Argon," AIAA Paper 71-157, New York, N. Y., 1971.

25. Sovey, J. S., "A 30-cm Diameter Argon Ion Source," Proposed AIAA Paper 76-1017, Key Biscayne, Fla., 1976.

26. Nakanishi, S. and Pawlik, E. V.; "Environmental Investigation of a 1.5-M-Diameter Kaufman Thruster," AIAA Paper 67-725, Colarado Springs, Colo., 1967.

27. Green, W. V., Smith, M. C., and Olson, D. M.: "Short-Time Creep-Rupture Behavior of Molybdenum at High Temperatures," Transactions of the Metallurgical Society of AIME, Vol. 215, 1959, pp. 1061-1066.

28. Carvalhinhos, H. and Argent, B. B., "The Creep of Molybdenum," Journal of the Institute of Metals, Vol. 95, 1967, pp. 364-368.

29. Rawlin, V. K., Banks, B. A., and Byers, D. C., "Design, Fabrication, and Operation of Dished Accelerator Grids on a 30-cm Ion Thruster." AIAA Paper 72-486, Bethseda, Md., 1972.

30. Byers, D. C.: "An Experimental Investigation of a High-Voltage Electron-Bombardment Ion Thruster. Journal of the Electrochemical Society, Vol. 116, 1969, pp. 9-17.

31. "8-cm Mercury Ion Thruster System Technology," AIAA Paper 74-1116, San Diego, Calif., 1974.

32. Cake, J. E., et al.: "Modular Thrust Subsystem Approaches to Solar Electric Propulsion Module Design," Proposed AIAA Paper 76-1062, Key Biscayne, Fla., 1976.

33. "A Forecast of Space Technology, 1980-2000," NASA SP-387, 1976.

34. Stover, J. B.; "System Tests with Electric Thruster Beam and Accelerator Directly Powered from Laboratory Solar Arrays," NASA TM X-3353, 1976.

35. Sater, B. L.; "The Advantages of the High Voltage Solar Array for Electric Propulsion," AIAA Paper 73-1103, Lake Tahoe, Nev., 1973.

36. Gooder, S.: NASA Lewis Research Center, Cleveland, Ohio, Private Communication, 1976.

TABLE I. - ON-ORBIT PROPULSION REQUIREMENTS[13]

Control requirement	Propellant flowrate, kg/yr	Number of standard 30-cm thrusters required per year
Station keeping		
Longitude drift	726	>15
Inclination drift	6673	136
Solar pressure		
Altitude drift	2315	47
Ellipticity drift	0 (14, 883)*	0 (303)*
Microwave pressure	31	1
Attitude control		
Gravity gradient	13, 804	281
Antenna control	74	2
Solar pressure	394	8
Microwave pressure	132	3
Totals	24, 129 (39, 032)*	493 (796)*

*Required after 15 satellites in orbit

TABLE II. - SEA LEVEL ATMOSPHERIC CONSTITUENCY[19]

Gas	Mol. fraction	Estimated total in atmosphere, kg
Nitrogen (N_2)	78.09	4.06×10^{18}
Oxygen (O_2)	20.95	1.09×10^{18}
Argon (A)	0.93	4.84×10^{16}
Carbon dioxide (CO_2)	0.03	1.56×10^{15}
Neon (Ne)	1.8×10^{-3}	9.36×10^{13}
Helium (He)	5.24×10^{-4}	2.72×10^{13}
Krypton (Kr)	1×10^{-4}	5.2×10^{12}
Hydrogen (H_2)	5.0×10^{-5}	2.6×10^{12}
Xenon (Xe)	8.0×10^{-6}	4.16×10^{11}
Ozone (O_3)	1.0×10^{-6}	5.2×10^{10}
Radon (Rn)	6.0×10^{-18}	3.12×10^{-1}

TABLE III. - PROPELLANT COST

Gas	Normalized cost / Liquified mass
Argon	1
Krypton	488
Xenon	1100

TABLE IV. - COMPONENT MASSES FOR 20,000 KG ARGON THERMODYNAMIC CRYOGENIC STORAGE SYSTEM[22]

Component	Mass, kg
Girth ring	141
Tank	45
Shield	69
Multi-layer insulation	48
Vacuum jacket	340
Internal support	5
Contingency	90
Subtotal	738
Propellant	20,000
Total	20,738

TABLE V. - THRUSTER INPUT POWER SUMMARY

Parameter	30-cm Mercury thruster	60-cm Argon thruster	
Specific impulse, sec	2840	8770	13000
Beam power, kW	2.2	184.2	405.0
Discharge power, kW	0.4	16.2	16.2
Fixed power, kW	0.05	0.1	0.1
Total power, kW	2.65	200.5	42.13

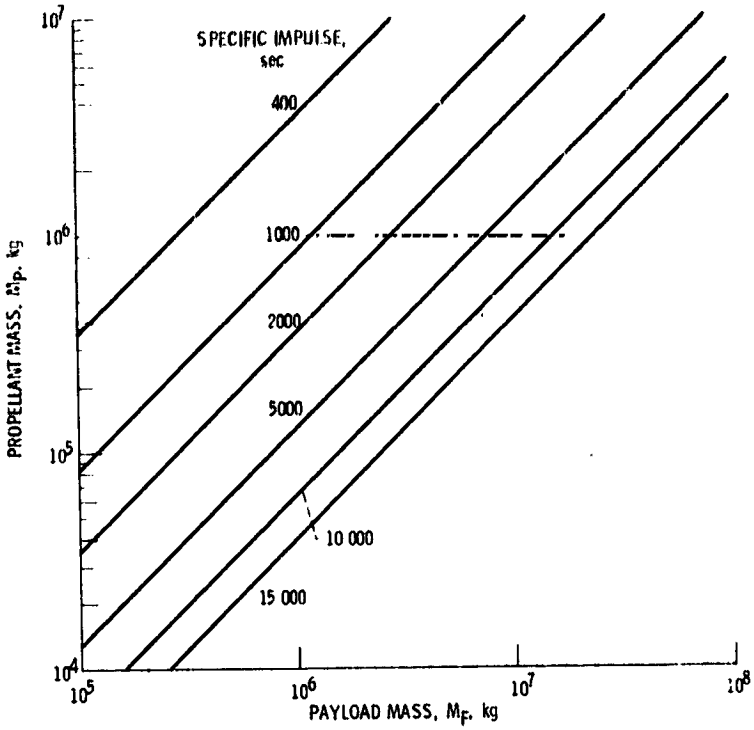

Figure 1. - Propellant mass as a function of payload mass for orbit transfer from 352 km to synchronous altitude with a 28.5^0 plane change and velocity increment of 5.77 km/sec.

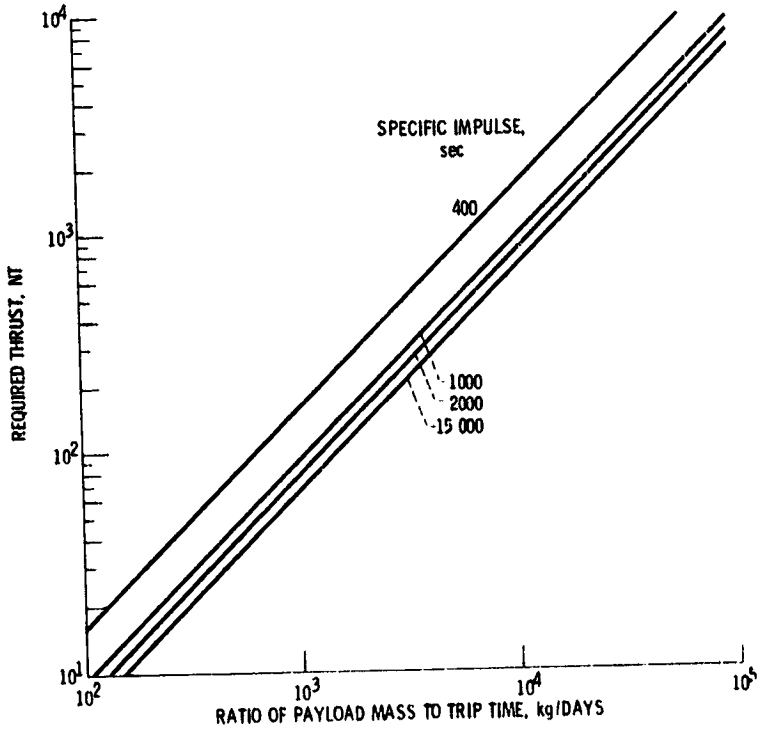

Figure 2. - Required thrust as a function of the ratio of payload mass to trip time for the conditions of figure 1.

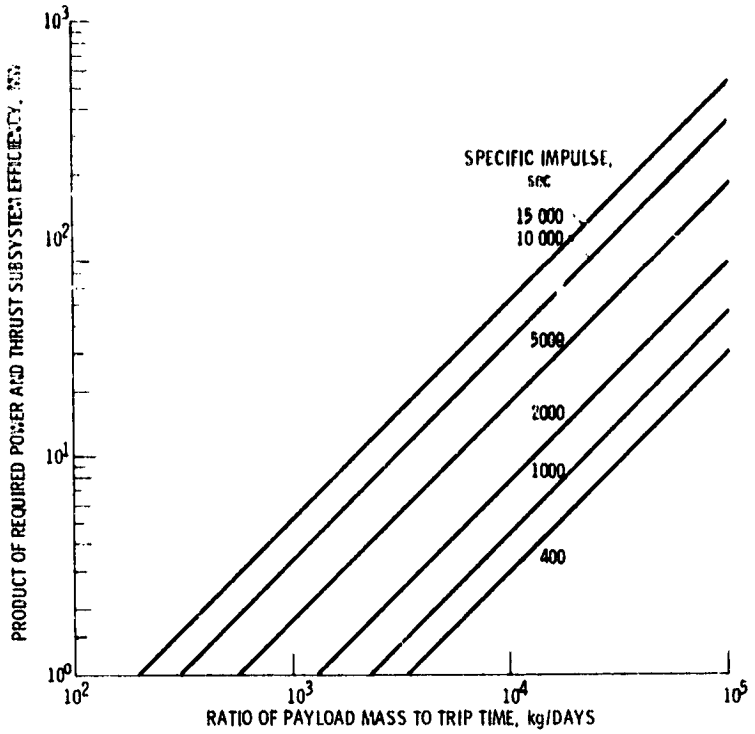

Figure 3. - Product of required power and thrust subsystem efficiency as a function of the ratio of payload mass to trip time for the conditions of figure 1.

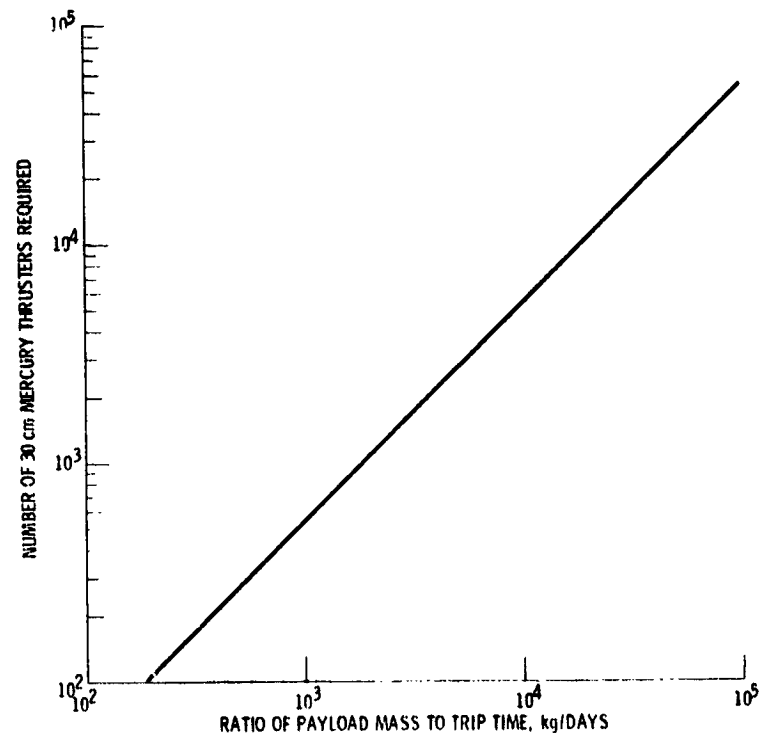

Figure 4. - Number of 30 cm mercury thrusters required as a function of the ratio of payload mass to trip time for the conditions of figure 1. Specific impulse of 2840 sec, and propellant utilization efficiency of 0.9.

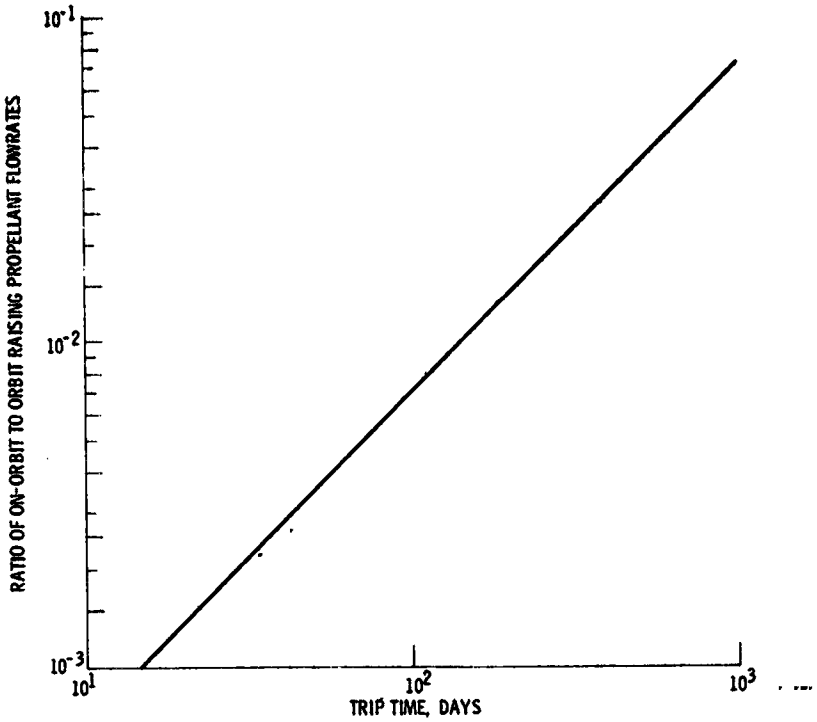

Figure 5. - Ratio of the propellant flowrates for on-orbit and orbit raising propulsion as a function of the orbit transfer time for a payload mass of 11.4×10^{6} kg, specific impulse of 13 000 sec.

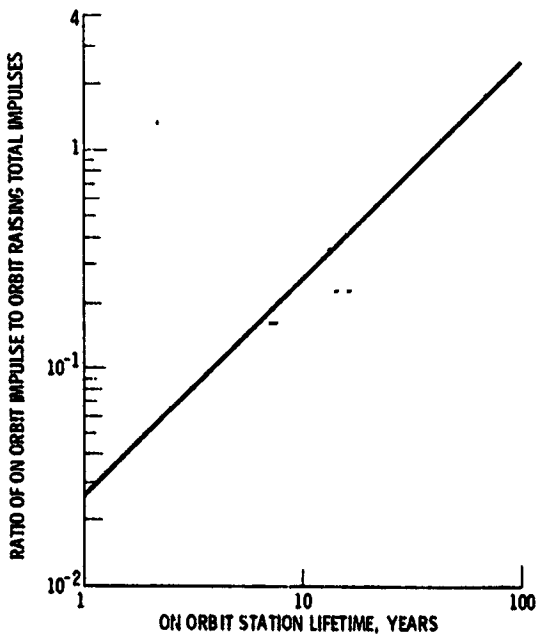

Figure 6. - Ratio of the total impulses for on orbit and orbit raising propulsion as a function of on-orbit station lifetime for the conditions of figure 5.

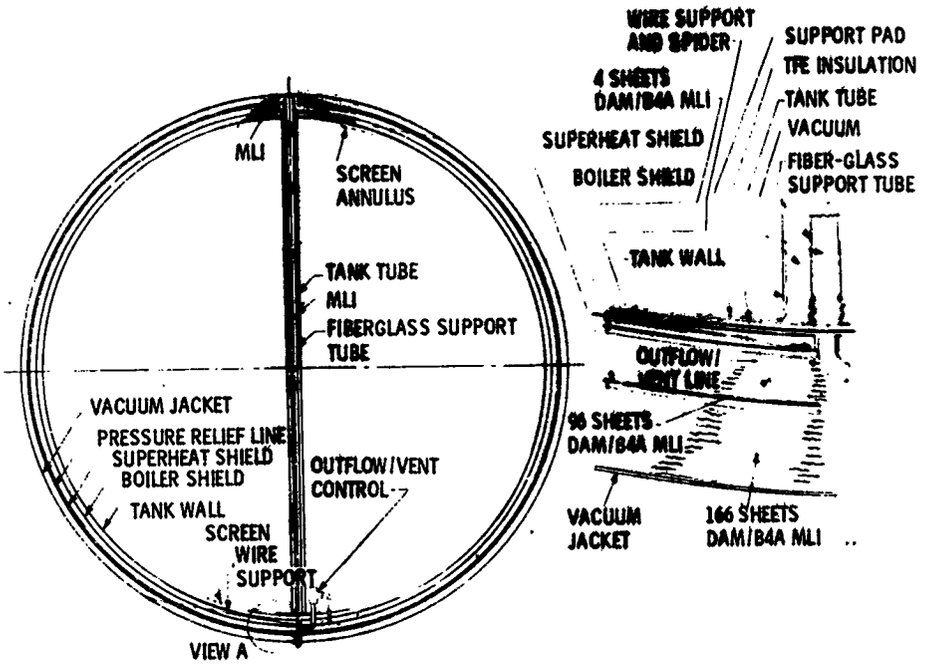

Figure 7. - Thermodynamic vent/screen storage system.

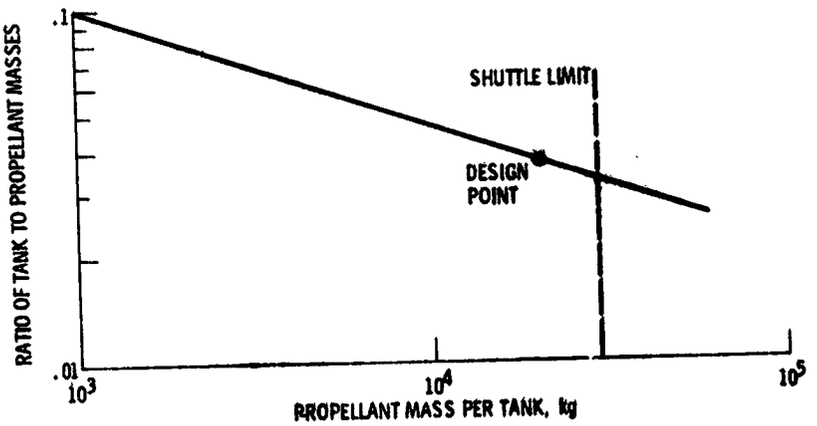

Figure 8. - Ratio of tank to propellant masses as a function of the propellant mass per tank.

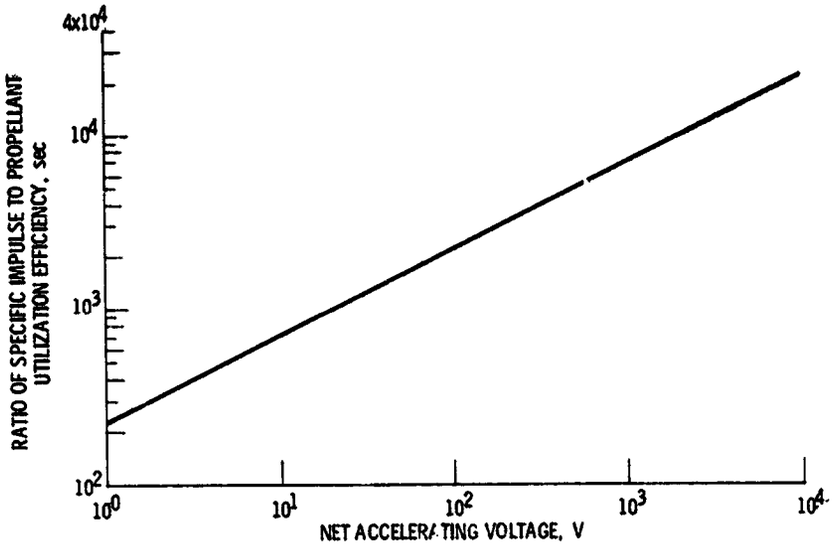

Figure 9. - Ratio of specific impulse to propellant utilization efficiency as a function of net accelerating voltage for argon.

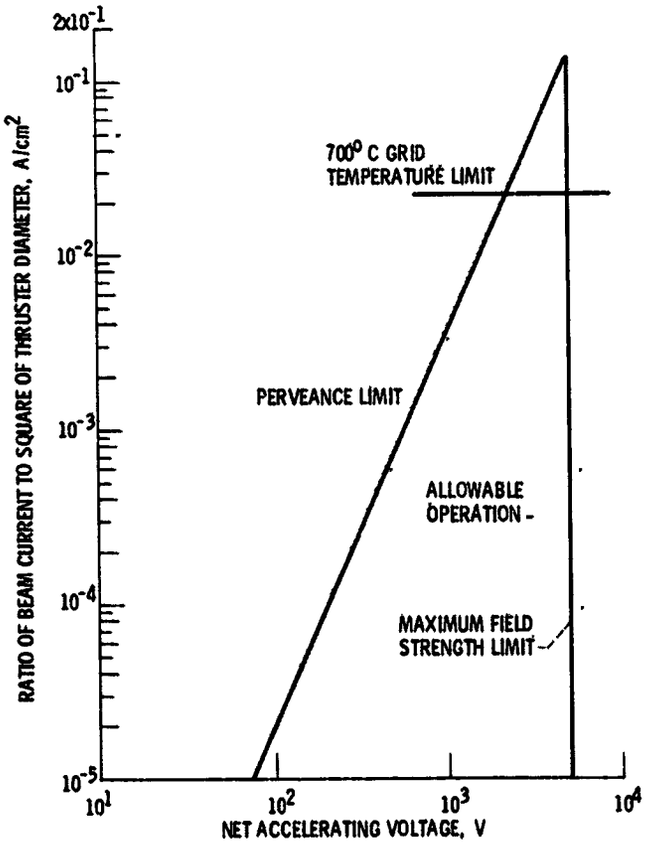

Figure 10. - Ratio of beam current to the square of thruster diameter as a function of the net accelerating voltage.

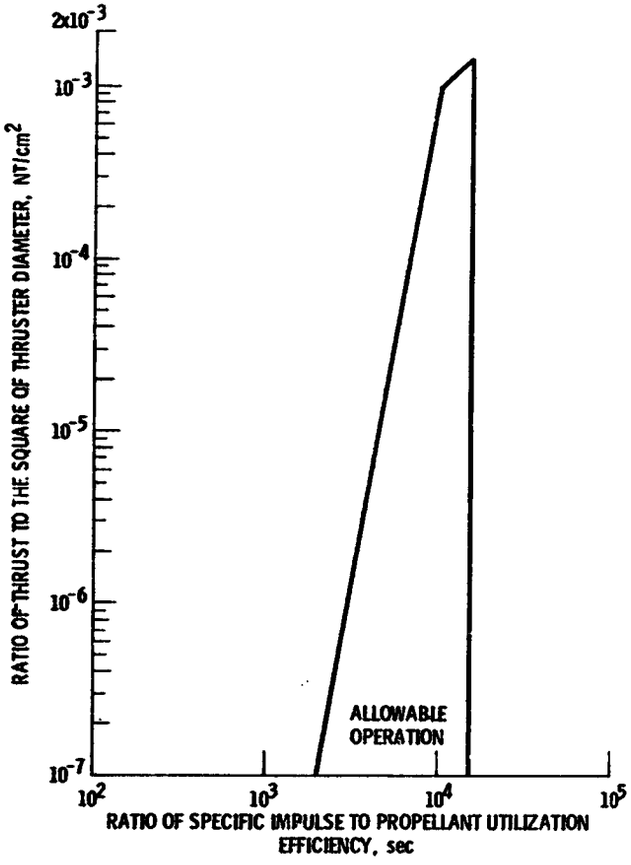

Figure 11. - Ratio of the thrust to the square of thruster diameter as a function of the ratio of the specific impulse to propellant utilization efficiency.

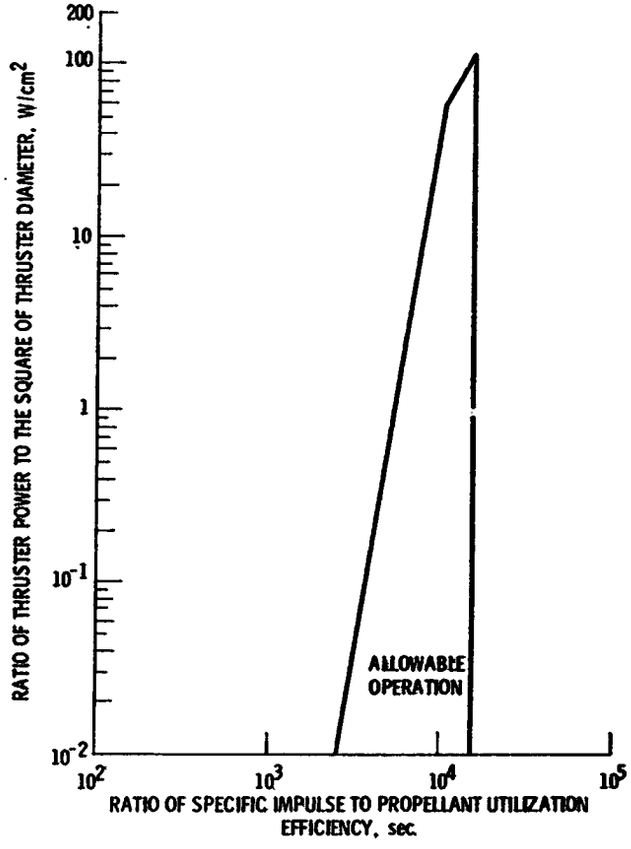

Figure 12. - Ratio of thruster power to the square of thruster diameter as a function of the ratio of specific impulse to propellant utilization efficiency.

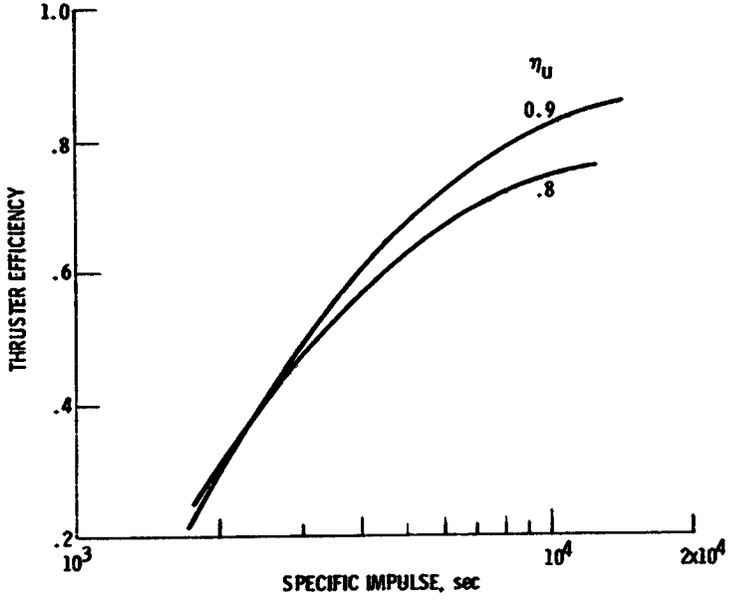

Figure 13. - Argon thruster efficiency as a function of specific impulse.

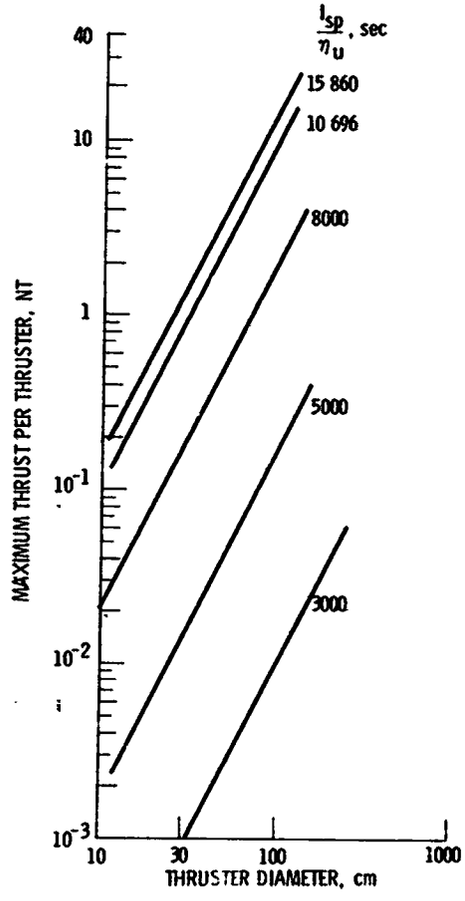

Figure 14. - Maximum thrust per thruster as a function of thruster diameter. Argon propellant.

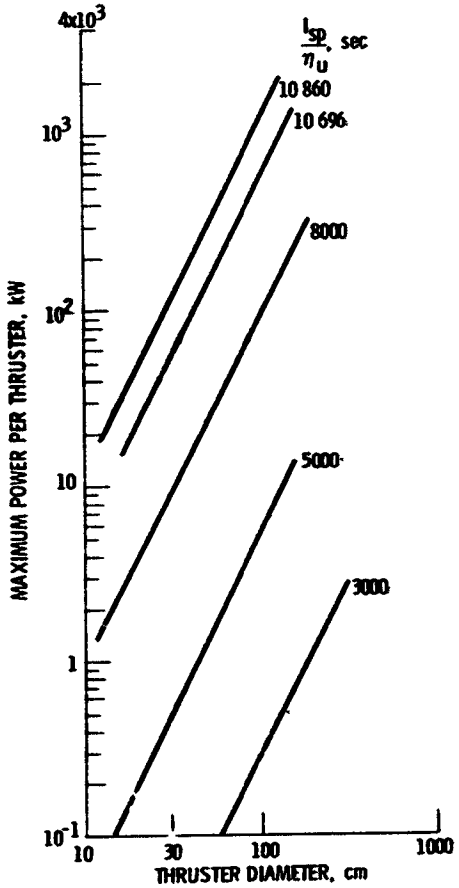

Figure 15. - Maximum power per thruster as a function of thruster diameter. Argon propellant.

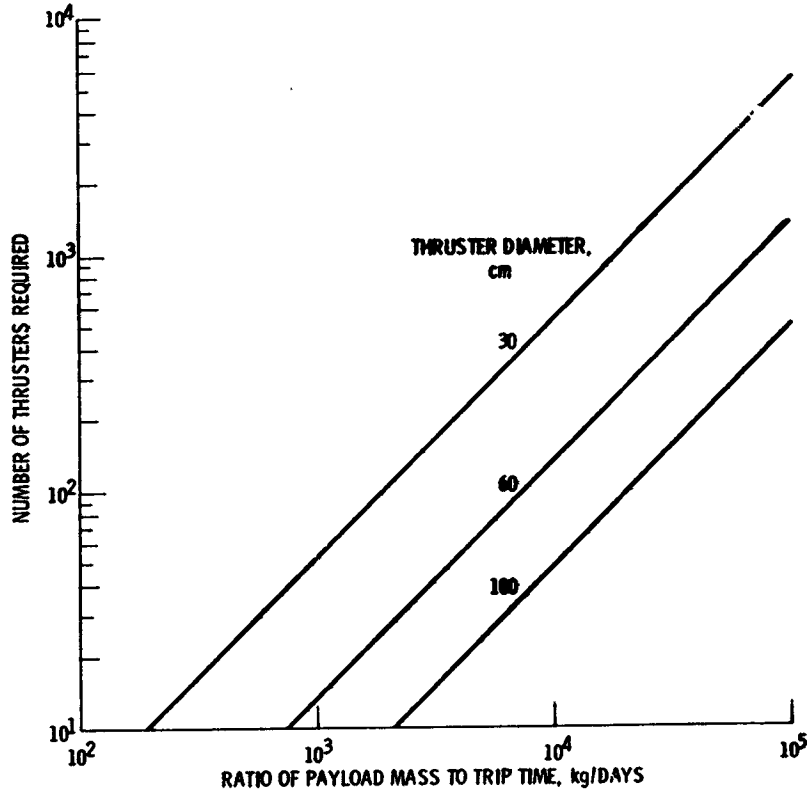

Figure 16. - Number of argon thrusters required as a function of the ratio of payload mass to trip time for the conditions of figure 1. Specific impulse of 13 000 sec and propellant utilization efficiency of 0.82.

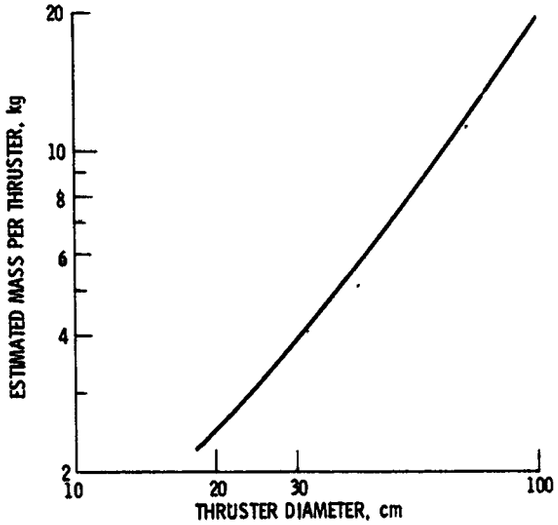

Figure 17. - Estimated mass of argon thruster as a function of thruster diameter.